Methods S1: Model implementation, related to STAR Methods MODEL IMPLEMENTATION

Models of single neurons and the network were developed using the parallel NEURON 7.4 simulator (Carnevale and Hines, 2006), and simulations were run with a fixed time step of 25 μ s.

Mathematical equations for voltage-dependent ionic currents: The dynamics for each compartment (soma or dendrite) followed the Hodgkin-Huxley formulation as previously described (Kim et al., 2013) in eqn. 1,

$$C_m dV_s / dt = -g_L (V_s - E_L) - g_c (V_s - V_d) - \sum I_{cur,s}^{int} - \sum I_{cur,s}^{syn} + I_{inj}$$
(1)

where V_s/V_d are the somatic/dendritic membrane potential (mV), $I_{cur,s}^{int}$ and $I_{cur,s}^{syn}$ are the intrinsic and synaptic currents in the soma, I_{inj} is the electrode current applied to the soma, C_m is the membrane capacitance, g_L is the conductance of the leak channel, and g_c is the coupling conductance between the soma and dendrite (similar term added for other dendrites connected to the soma). The intrinsic current $I_{cur,s}^{int}$, was modeled as $I_{cur,s}^{int} = g_{cur}m^ph^q(V_s - E_{cur})$, where g_{cur} is its maximal conductance, *m* its activation variable (with exponent *p*), *h* its inactivation variable (with exponent *q*), and E_{cur} its reersal potential (a similar equation is used for the synaptic current $I_{cur,s}^{syn}$ but without *m* and *h*). The kinetic equation for each of the gating variables *x* (*m* or *h*) takes the form but without *m* and *h*). The kinetic equation for each of the gating variables *x* (*m* or *h*) takes the form

$$\frac{dx}{dt} = \frac{x_{\infty} \left(V, \left[Ca^{2+} \right]_i \right) - x}{\tau_x \left(V, \left[Ca^{2+} \right]_i \right)} \quad (2)$$

where x_{∞} is the steady state gating voltage- and/or Ca²⁺- dependent gating variable and τ_x is the voltage- and/or Ca²⁺- dependent time constant. The equation for the dendrite follows the same format with 's' and 'd' switching positions in eqn. 1.

Principal neuron (PN) models: PN had five compartments: soma (diameter 24.75 μ m, length 25 μ m), an apical dendrite (a-dend; diameter 3 μ m; length 270 μ m), another dendrite (p-dend; diameter 5 μ m; length 555 μ m) to match passive properties, an axon initial segment (AIS; diameter 0.5 μ m; length 50 μ m), and an axon (diameter 0.5 μ m; length 100 μ m). Values of specific membrane resistance, membrane capacity and cytoplasmic (axial) resistivity were,

respectively, $R_m = 40 \pm 5 \text{ k}\Omega\text{-cm}^2$, $C_m = 1.5 \mu\text{F/cm}^2$, and $R_a = 150 \Omega\text{-cm}$. Leakage reversal potential (E_L) was set to -75 ± 4 mV. The resulting V_{rest} was -66 ± 4 mV, input resistance $(R_{\rm IN})$ was 140 ± 20 MΩ, and time constant $(\tau_{\rm m})$ was ~30 ms, all of which were within the ranges reported in previous physiological studies (Washburn and Moises, 1992). Soma and dendrite compartments had the following currents: leak (I_L), voltage-gated persistent muscarinic ($I_{\rm M}$), high-voltage activated Ca²⁺ ($I_{\rm Ca}$), spike-generating sodium ($I_{\rm Na}$), potassium delayed rectifier (I_{DR}) , A-type potassium (I_A) (Li et al., 2009; Power et al., 2011) and hyperpolarization-activated nonspecific cation (I_h) current. In addition, the soma had a slow apamin-insensitive, voltage-independent afterhyperpolarization current (I_{sAHP}) (Alturki et al., 2016; Power et al., 2011). The axonal compartments had the following currents: leak (I_L) , high-threshold sodium ($I_{Na1.2}$), low-threshold sodium ($I_{Na1.6}$), and potassium delayed rectifier (IDR) (Hu et al., 2009). See Tables S1 and S2 for equations of current kinetics and maximal densities. Based on firing patterns observed in slices, PNs in the model had Type-A (adapting) and Type C (continuous) generated by adjusting magnitude of Ca²⁺-dependent K⁺ current, either 50 or 0.2 mS/cm², respectively (Kim et al., 2013). PN models contained properties for low- and high- threshold oscillation to mimic physiological parameters as closely as possible (Feng et al., 2016; Kim et al., 2013; Li et al., 2009; Pape et al., 1998).

Interneuron (IN) models: Since most INs sampled in experiments showed fast-spiking Int (FSI) characteristics they were modelled as FSI. The IN model contained five compartments; a soma (diameter 10 μ m; length 20 μ m) and four dendrites (diameter 3 μ m; length 100 μ m). Each compartment contained a fast Na⁺ (I_{Na}) and a delayed rectifier K⁺ (I_{DR}) current. Network contains two types of INs: (a) Basket INs that target PN at the soma, and (b) Chandelier IN (Chn) that target PN at the AIS. Both models reproduced APs with short half-width (<1 ms). Passive membrane properties of Basket INs and Chns were Rm = 10 ± 1 and 15 ± 1 kΩ-cm², C_m = 1.4 and 0.8 μ F/cm², R_a = 100 and 100 Ω-cm, respectively.

Network size and cell type proportions: To model a 400 μ m (1.4 x 1.4 x 0.4 mm) basal amygdala slice, we generated 20,572 neurons with cellular composition of 40% PN_A (n=8,229), 40% PN_C (n=8,229), 18% Basket INs (n=3,702), and 2% Chandelier INs (n=411). *Mathematical equations for synaptic currents:* All excitatory transmission was mediated by AMPA/NMDA receptors, and inhibitory transmission by GABA_A receptors. The corresponding synaptic currents were modelled by dual exponential functions (Destexhe et al., 1994; Durstewitz et al., 2000) as shown in eqns. 3-5,

$$I_{AMPA} = w \times G_{AMPA} \times (V - E_{AMPA})$$

$$G_{AMPA} = g_{AMPA,max} \times F_{AMPA} \times r_{AMPA}$$

$$r_{AMPA}' = \alpha Tmax_{AMPA} \times ON_{AMPA} \times (1 - r_{AMPA}) - \beta_{AMPA} \times r_{AMPA}$$
(3)

$$I_{NMDA} = w \times G_{NMDA} \times (V - E_{NMDA})$$

$$G_{NMDA} = g_{NMDA,max} \times F_{NMDA} \times s(V) \times r_{NMDA}$$

$$r_{NMDA}' = \alpha T max_{NMDA} \times ON_{NMDA} \times (1 - r_{NMDA}) - \beta_{NMDA} \times r_{NMDA}$$
(4)

$$I_{GABAa} = w \times G_{GABAa} \times (V - E_{GABAa})$$

$$G_{GABAa} = g_{GABAa,max} \times F_{GABAa} \times r_{GABAa}$$

$$r_{GABAa}' = \alpha Tmax_{GABAa} \times ON_{GABAa} \times (1 - r_{GABAa}) - \beta_{GABAa} \times r_{GABAa}$$
(5)

where *V* is the membrane potential (mV) of the compartment (dendrite or soma) where the synapse is located, *I* is the current injected into the compartment (nA), *G* is the synaptic conductance (μ S), *w* is the synaptic weight (unitless), and *E* is the reversal potential of the synapse (mV). *g_{x,max}* is the maximal conductance (μ S), *F* implements short-term plasticity as defined in the next section, and *r_x* determines the synaptic current rise and decay time constants based on the terms $\alpha Tmax$ and β (Destexhe et al., 1994). The voltage-dependent variable *s*(*V*) which implements the Mg²⁺ block was defined as: *s*(*V*) = [1 + 0.33 exp(-0.06 *V*)]⁻¹ (Zador et al., 1990). The terms *ON_{NMDA}* and *ON_{AMPA} are set* to 1 if the corresponding receptor is open, else to 0. Synaptic parameter values are listed in Table S3 as mean \pm SD. For all connections, synaptic weight *w* was distributed log-normally with a cut off of three times the mean to prevent non-physiological values.

Short-term presynaptic plasticity: The term Int represents both Chns and Basket INs. All model AMPA and GABA synapses also exhibited short term pre-synaptic plasticity (Kim et al., 2013). Short-term depression was modelled at Int->PN and PN->Int connections based on experimental findings in this study and previous reports (Woodruff and Sah, 2007). Short term plasticity was implemented as follows (Hummos et al., 2014): For facilitation, the factor F was calculated using the equation: $\tau_F * dF/dt = 1 - F$ and was constrained to be ≥ 1 . After each stimulus, F was multiplied by a constant, f (≥ 1) representing the amount of facilitation per pre-synaptic action potential and updated as F \rightarrow F*f. Between stimuli, F recovered exponentially back toward 1. A similar scheme was used to calculate the factor D for depression: τ_D *dD/dt=1-D and D constrained to be ≤ 1 . After each stimulus, D was multiplied by a constant d (≤ 1) representing the amount of depression per pre-synaptic action potential to be ≥ 1 . After each stimulus, D was multiplied by a constant d (≤ 1) representing the amount of depression per pre-synaptic action potential and updated as D \rightarrow D*d. Between stimuli, D recovered exponentially back toward 1. We modelled depression using two factors d1 and d2 with d1 being fast and d2 being slow subtypes, and d=d_1*d_2 and was constrained to be ≥ 1 . After each stimulus, F was

multiplied by a constant, $f (\geq 1)$ representing the amount of facilitation per pre-synaptic action potential and updated as $F \rightarrow F^*$. Parameters for modelling short-term plasticity are listed in Table S4. Our model did not have long-term synaptic plasticity.

Intrinsic connections: Except for Int->Int connectivity that had both chemical and electrical components, all other connections were via chemical synapses; hereafter, unless qualified by 'electrical', the connections are assumed to be via chemical synapses. PN->PN connections were not detected in our data set and so were not included. For all the other connection types, we used published data (Woodruff and Sah, 2007), limiting connectivity from/to INs to within ~300 µm. Using such data, probabilities in the model for unidirectional Int->PN and PN->Int synaptic connections, and for Int->Int electrical connections were, respectively, 34%, 12%, and 8%. Also, reciprocal connections between PNs and INs was set to 16%. These connectivity of 26% of which 20% was unidirectional and 3% bi-directional. Chns contacted only PNs so there were no Chn->Chn or Chn->Basket IN connections. These probabilities resulted in the intrinsic connectivity shown in Table S4. Axonal conduction delay was distance-dependent using a conduction velocity of 500 µm/ms.

Calculation of LFP: We first recorded transmembrane ionic currents from each compartment of the model cells using the *extracellular mechanism* in NEURON (Carnevale and Hines, 2006; Parasuram et al., 2016). The extracellular potential arising from each neuronal compartment was then calculated using the line source approximation method, which provides a better approximation than using point sources (Gold et al., 2006; Schomburg et al., 2012). The extracellular potential of a line compartment was estimated as

$$\phi_{EP} = \frac{l}{4\pi\sigma\Delta s} \log |\frac{\sqrt{h^2 + r^2} - h}{\sqrt{l^2 + r^2} - l}| \quad (6)$$

where, *I* denotes the transmembrane current from just that compartment, Δs the length of the line compartment, *r* the radial distance from the line, *h* the longitudinal distance from the end of the line, and $l = \Delta s + h$ the distance from the start of the line (Parasuram et al., 2016). We chose conductivity σ of the extracellular medium as 0.3 S/m (Einevoll et al., 2013; Goto et al., 2010). The individual extracellular potentials were summed linearly (Linden et al.,

2014) at 0.5 ms resolution, to obtain ϕ_{LFPs} (eqn.7) as the LFP for an *N*-neuron network with *n*-compartment-cells.

$$\phi_{LFPs} = \sum_{N=1}^{N_neurons} \sum_{i=1}^{n_source} \frac{I_{Ni}}{4\pi\sigma\Delta s_{N_i}} \log \left| \frac{\sqrt{h_{N_i}^2 + r_{N_i}^2 - h_{N_i}}}{\sqrt{l_{N_i}^2 + r_{N_i}^2} - l_{N_i}} \right|$$
(7)

where N_i denotes i^{th} compartment of N^{th} neuron in the network.

Conduction delays: Conduction delays between cells were calculated and assigned in a distance-dependent manner:

$$D = \frac{\sqrt{(x_1 - x_2)^2 + (y_1 - y_2)^2 + (z_1 - z_2)^2}}{A_V}$$
(8)

Where (x_1, y_1, z_1) and (x_2, y_2, z_2) are the coordinates of the pre and postsynaptic cells, respectively. A_V is the axonal conduction velocity (0.5 m/s).

Analytical model to predict SW profile: Using a log-normal distributions of connection probabilities and synaptic strengths, analytical equations were developed to predict the numbers of PNs, Chns, and Baskets that fire during each cycle of the ripple, as designated as PN(n), Chn(n) and BC(n), respectively. These numbers then provide an estimate of the SW profile.

$$PN(n) = Chn(n-1) * E_{Chn \to PN} - BC(2n-1) * I_{PV \to PN} * \alpha(n)$$
(9)
$$E_{Chn \to PN} = 2.9, I_{PV \to PN} = 1.35, \alpha(n) = [1,1,1,1,1,2,1.6,1.8,2.0]$$

$$Chn(n) = PN(n-1) * E_{PN \to Chn} - BC(n-1) * I_{PV \to Chn} * \beta(n) (10)$$
$$E_{PN \to Chn} = 1.3, I_{PV \to Chn} = 0.42, \beta(n) = [1,1,1,1,1,1,1,9,1.9,2.0]$$

$$BC(n) = PN(n-1) * E_{PN \to PV} - BC(n-1) * I_{PV \to PV} * \gamma(n) (11)$$
$$E_{PN \to PV} = 1.1, I_{PV \to PV} = 0.69, \gamma(n) = [1,1,1,1,1,1,1,1,2,1,2]$$
$$PN_a(0) = 0; Chn(0) = 1; BC(0) = 0,$$

where PN(n), Chn(n), and BC(n) represent the number of PNs, Chns, and Basket cells activated at the nth interval; $E_{X \to Y}$ is the number of Y neurons activated by each X neuron; $I_{X \to Y}$ is the number of Y neurons inhibited by each X neuron; $\alpha(n)$, $\beta(n)$, $\gamma(n)$ are functions that represent summation of inhibition over time.

The parameters E_x->y were computed by multiplying the percent of synaptic weights that were above threshold (minimum weight that would fire a postsynaptic cell) by the total number of excitatory connections made from cell type x to cell type y. I_x->y was found in the same way, by setting a threshold for strong inhibition and multiplying the percent of synaptic weights above that threshold by the total number of inhibitory connections made from cell type x to cell type y. The functions alpha, beta, and gamma were assumed to start at 1 and increase over time, representing temporal summation for inhibition. The specific values were chosen to be between 1 and 2 and had to be tuned.

Current Type	Gating Variable	α	β	x_{∞}	τ_x (ms)	
T 1	<i>p</i> =3	$\frac{-0.4(V+30)}{\exp[-(V+30)/7.2]-1}$	$\frac{0.124(V+30)}{\exp[(V+30)/7.2]-1}$	$\frac{\alpha}{\alpha+\beta}$	$\frac{0.6156}{\alpha + \beta}$	
$I_{Na}{}^{l}$	q=l	$\frac{-0.03(V+45)}{\exp[-(V+45)/1.5]-1}$	$\frac{0.01(V+45)}{\exp[(V+45)/1.5]-1}$	$\frac{1}{\exp[(V+50)/4]+1}$	$\frac{0.6156}{\alpha + \beta}$	
I_{Kdr}^{l}	p=l	exp[-0.1144(V + 15)]	exp[-0.0801(V + 15)]	$\frac{1}{\exp[(-V - 15)/11] + 1}$	$\frac{50*\beta}{1+\alpha}$	
I_{H}^{2}	q=l	exp[0.0832(V + 75)]	exp[0.0333(V + 75)]	$\frac{1}{\exp[(V+81)/8]+1}$	$\frac{\beta}{0.0081(1+\alpha)}$	
I_{KM}^{3}	<i>p</i> =2	$\frac{0.016}{\exp[-(V+52.7)/23]}$	$\frac{0.016}{\exp[(V + 52.7)/18.8]}$	$\frac{1}{\exp[(-V - 52.7)/10.3] + 1}$	$\frac{1}{\alpha + \beta}$	
I_{Ca}^{3}	<i>p</i> =2	_	_	$\frac{1}{\exp[(-V - 30)/11] + 1}$	$\frac{2.5}{\exp\left[\frac{-(V+37.1)}{32.3}\right] + \exp\left[\frac{(V+37.1)}{32.3}\right]}$	
ICa	q=l	_	_	$\frac{1}{\exp[(V+12.6)/18.9]+1}$	420	
$I_{Nap}{}^4$	<i>p</i> =1	_	_	$\frac{1}{\exp[(-V-48)/5]+1}$	$2.5 + 14 * \exp[- V + 40 /10]$	
I _{sAHP} ³	<i>p</i> =1	$\frac{0.0048}{\exp[-5\log_{10}([Ca]_{i2})-17.5]}$	$\frac{0.012}{\exp[2\log_{10}([Ca]_{i2})+20]}$	$\frac{\alpha}{\alpha+\beta}$	48	
I 5	<i>p=3</i>	$\frac{-0.182(V+30)}{\exp[-(V+30)/7]-1}$	$\frac{0.124(V+30)}{\exp[(V+30)/7] - 1}$	$\frac{\alpha}{\alpha+\beta}$	$\frac{1}{\alpha + \beta}$	
I _{Na1.2} 5	q=l	$\frac{-0.024(V+50)}{\exp[-(V+50)/5]-1}$	$\frac{0.0091(V+75)}{\exp[(V+75)/5]-1}$	$\frac{1}{\exp[(V+72)/6.2]+1}$	$\frac{1}{\alpha + \beta}$	
I _{Na1.6} 5	<i>p=3</i>	$\frac{-0.182(V+43)}{\exp[-(V+30)/6]-1}$	$\frac{0.124(V+43)}{\exp[(V+30)/6]-1}$	$\frac{\alpha}{\alpha+\beta}$	$\frac{1}{\alpha + \beta}$	
	q=l	$\frac{-0.024(V+50)}{\exp[-(V+50)/5]-1}$	$\frac{0.0091(V+75)}{\exp[(V+75)/5]-1}$	$\frac{1}{\exp[(V+72)/6.2]+1}$	$\frac{1}{\alpha + \beta}$	

Table 1. Gating parameters of ion channels.

1: (Migliore et al., 1999), 2 : (Magee et al., 1998), 3 : (Kim et al., 2013), 4 -:(Traub et al., 2003), 5 - :(Hu et al., 2009).

	Chandelier interneuron		Basket interneuron		Type A Principal neuron		Type C Principal neuron			
	soma	dendrites	soma	dendrites	soma	dendrites	axon	soma	dendrites	axon
Cm	0.8	0.8	1.4	1.4	1.5	1.5	0.4	1.5	1.5	0.4
$(\mu F/cm^2)$										
Ra (Ωcm)	100	100	100	100	150	150	150	150	150	150
Conductance										
(mho/cm^2)										
gNabar	0.09	0.024	0.156	7.82e-3	0.015	0.015	**	0.015	0.015	**
gKdrbar	6	0.0011	0.010	2.77e-3	0.002	0.002	0.00	0.002	0.002	0.002
gLeak	0.00	0.0001	3	1.5e-4	4.8e-5	4.8e-5	2	4.8e-5	4.8e-5	0.001
gNapbar	45		1.5e-4		5.59e-	5.59e-4	0.00	5.59e-	5.59e-4	
gHdbar	0.00				4	1.5e-5	1	4	1.5e-5	
gCabar	01				1.5e-5	5.5e-4		1.5e-5	5.5e-4	
gMbar					5.5e-4	2.2e-3		5.5e-4	2.2e-3	
gsAHPbar					2.2e-3	0.05		2.2e-3	0.0002	
gKapbar					0.05	0.002		0.0002	0.002	
					0.002			0.002		

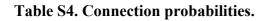
Table 2. Parameters of single cell models.

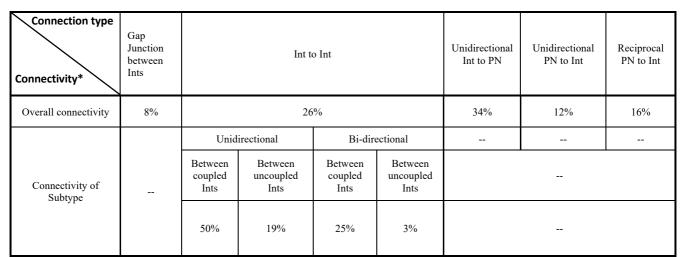
** Sodium channel densities were exponentially distributed along the axon as in Hu et al (Hu et al., 2009).

Table 3. Parameters of synapse models.

Pre-Post	AMPA/NMDA reversal potential (mV) and rise/decay time constant (ms) and conductance (uS)	GABA reversal potential (mV) and rise/decay time constants (ms) and conductance (uS)	Peak Synaptic Current (pA)
Chn – PN		-50 mV; Rise: 0.83 ms; Decay: 6.27 ms; 3.0e-3 uS (Veres et al., 2014)	41 ± 35 (Galarreta and Hestrin, 1997)
Bask – PN		-70 mV; Rise: 0.3 ms; Decay: 7.5 ms; 8e-3 uS (Galarreta and Hestrin, 1997)	39 ± 9 (Galarreta and Hestrin, 1997)
PN - PN			
PN - Chn	0 mV; Rise: 0.88 ms; Decay: 2.3 ms; 2.35e-3 uS		144.4 ± 107.7
Bask - Chn*		-70 mV; Rise: 1.1 ms; Decay: 6.8 ms; 8e-3 uS	39 ± 9
Chn – Chn		Gap junction coupling coeff. 0.2 (unitless)	
Bask – Bask		-70 mV; Rise: 1.1 ms; Decay: 6.8 ms; 4e-3 uS Gap junction coupling coeff. 0.2 (unitless) (Woodruff and Sah, 2007)	39 ± 9 (Woodruff et al., 2006)
Chn – Bask			
PN - Bask	0 mV; Rise: 0.69 ms; Decay: 1.83 ms; 2.0e-3		139.9 ± 75.95

* - Unknown. Assumed similar to Bask-Bask.





* All values from Woodruff et al (Woodruff and Sah, 2007). Here, Int refers to both Basket Ints and Chandelier Ints with the exception that there are no Chandelier – Basket or Chandelier – Chandelier synapses.